Since January 2020 Elsevier has created a COVID-19 resource centre with free information in English and Mandarin on the novel coronavirus COVID-19. The COVID-19 resource centre is hosted on Elsevier Connect, the company's public news and information website.

Elsevier hereby grants permission to make all its COVID-19-related research that is available on the COVID-19 resource centre - including this research content - immediately available in PubMed Central and other publicly funded repositories, such as the WHO COVID database with rights for unrestricted research re-use and analyses in any form or by any means with acknowledgement of the original source. These permissions are granted for free by Elsevier for as long as the COVID-19 resource centre remains active.

Pathology - Research and Practice 236 (2022) 154000

Contents lists available at ScienceDirect

Pathology - Research and Practice

journal homepage: www.elsevier.com/locate/prp

Cell tropism and viral clearance during SARS-CoV-2 lung infection

Constantin Schwab *, Lisa Maria Domke, Fabian Rose, Ingrid Hausser, Peter Schirmacher, Thomas Longerich

Institute of Pathology, Heidelberg University Hospital, Heidelberg, Germany

ARTICLE INFO

Keywords:
SARS-CoV-2 infection
COVID-19
Cellular target
Time-course
Endothelialitis

ABSTRACT

Pulmonary capillary microthrombosis has been proposed as a major pathogenetic factor driving severe COVID-19. Autopsy studies reported endothelialitis but it is under debate if it is caused by SARS-CoV-2 infection of endothelial cells. In this study, RNA *in situ* hybridization was used to detect viral RNA and to identify the infected cell types in lung tissue of 40 patients with fatal COVID-19. SARS-CoV-2 Spike protein-coding RNA showed a steadily decreasing signal abundance over a period of three weeks. Besides the original virus strain the variants of concern Alpha (B.1.1.7), Delta (B.1.617.2), and Omicron (B.1.1.529) could also be detected by the assay. Viral RNA was mainly detected in alveolar macrophages and pulmonary epithelial cells, while only single virus-positive endothelial cells were observed even in cases with high viral load suggesting that viral infection of endothelial cells is not a key factor for the development of pulmonary capillary microthrombosis.

1. Introduction

Since late 2019 severe acute respiratory syndrome coronavirus 2 (SARS-CoV-2) has caused a global pandemic [12]. While most infected people experience a bland course with mild or no symptoms at all, some patients develop a more severe corona virus disease 2019 (COVID-19) necessitating hospitalization and in severe cases intensive care unit treatment with mechanical ventilation or extracorporal membrane oxygenation. Especially, elder people and patients with pre-existing co-morbidities are at risk to develop an acute respiratory distress syndrome [12]. As the SARS-CoV-2 genome seems to be in a hyper-mutating state, new virus variants are frequently detected and are responsible for the numerous waves of infection still keeping the world in suspense. During the last two pandemic years, several vaccines targeting the viral Spike protein have proven efficacy. In addition, medications either targeting the viral replication or acting as immunomodulators to prevent an overwhelming immune response have shown to reduce the likelihood of a fatal disease outcome. However, patients requiring mechanical ventilation still face a high risk of mortality. Thus, there is a need for deciphering the pathophysiology of COVID-19.

Several studies reported an endotheliopathy leading to increased permeability, edema, diffuse alveolar damage, hemorrhage and thrombosis [1,14,15]. While some authors claimed the detection of viral particles in infected (kidney) endothelial cells, others questioned these results and stated that structures normally found in the cytoplasm of a cell after conventional chemical fixation may be misinterpreted as viral particles [9,26]. In particular, it is still unclear whether SARS-CoV-2-related endotheliopathy is caused by viral infection of endothelial cells or by another indirect mechanism (*e.g. via* a cytokine storm related to strong activation of the immune system during COVID-19). Here, we analyzed the presence of viral RNA in lung tissue of COVID-19 patients over time and identified the infected cell types by dual-color RNA *in situ hybridization* (RNA-ISH).

2. Material and methods

2.1. Study cohort

All COVID-19 patients being referred to the Institute of Pathology, Heidelberg University Hospital for autoptic examination between March, 26th 2020 and February, 28th 2022 were registered in the COVID-19 autopsy and biomaterial registry Baden Wuerttemberg. SARS-CoV-2 infection was confirmed by reverse transcriptase polymerase chain reaction performed on nasopharyngeal swab samples

Abbreviations: ACE2, Angiotensin Converting Enzyme 2; CD68, CD68 molecule; COPD, chronic obstructive pulmonary disease; COVID-19, corona virus disease; FFPE, formalin-fixed, paraffin-embedded; ISH, *in situ* hybridization; KRT18, keratin 18; MCAM, melanoma cell adhesion molecule; RNA, ribonucleic acid; SARS-CoV-2, severe acute respiratory syndrome coronavirus 2; T2DM, type 2 diabetes mellitus; TMPRSS2, Transmembrane Serine Protease 2.

* Correspondence to: Institute of Pathology, Heidelberg University Hospital, Im Neuenheimer Feld 224, 69120 Heidelberg, Germany.
E-mail address: constantin.schwab@med.uni-heidelberg.de (C. Schwab).

https://doi.org/10.1016/j.prp.2022.154000
Received 1 April 2022; Received in revised form 23 June 2022; Accepted 29 June 2022
Available online 30 June 2022
0344-0338/© 2022 Elsevier GmbH. All rights reserved.

either before or during hospitalization or prior to autopsy in all patients. From this COVID-19 repository, 40 patients were selected based on the time interval between positive SARS-CoV-2 testing and death, which covered a period of one month. These included 12 patients infected by virus variants of concern. Lung tissue from autopsy cases before the COVID19 pandemic served as negative controls. The study was approved by the ethics committee of the University of Heidelberg Faculty of Medicine (no. S-242/2020) and carried out in accordance with the Declaration of Helsinki. According to the ethićs vote informed consent was not required.

2.2. Autopsies

All autopsies were performed applying a standardized protocol as described previously [13]. Tissue samples were fixed immediately after organ dissection using 4% neutral-buffered formalin. To optimize lung fixation, formalin was instilled in the trachea and the major pulmonary vessels. Lung dissection was performed after three days of fixation in a formalin-filled container of adequate size. Axial sections (slice thickness: 1 cm) were retrieved and photographically documented. Three representative tissue samples were taken from each pulmonary lobe for histological examination. Tissue samples were submitted to the tissue bank of the German Center for Infection Research.

2.3. Histology

For histological evaluation, 3-µm sections were retrieved from formalin-fixed, paraffin-embedded (FFPE) samples and stained according to standard protocols (hematoxylin and eosin, periodic acid Schiff reaction, and acid fuchsin orange G). The histological sections of the lungs were assessed by at least two pathologists (TL, CS). Histological changes were recorded in a standardized fashion as reported previously [13].

2.4. RNA in situ hybridization

RNA *in situ* hybridization (RNA-ISH) was performed on 5-µm thick sections of FFPE lung tissues using the RNAscope® platform according to the manufactureŕs instructions (Advanced Cell Diagnostics (ACD), Newark, CA, USA). For single detection of the Spike protein coding gene a SARS-CoV-2 specific probe (RNAscope® Probe V-nCoV2019-S, ACD Cat# 848561) was used together with a single detection kit (RNAscope® 2.5 HD Reagent Kit-RED, ACD, Cat# 322350). For dual RNA-ISH the duplex detection kit (RNAscope® 2.5 HD Duplex Reagent Kit, ACD, Cat# 322430) was used combining the SARS-CoV-2 specific probe and probes for Melanoma Cell Adhesion Molecule (MCAM, RNAscope® Probe Hs-MCAM-C2, ACD Cat# 601731-C2) to detect endothelial cells, keratin 18 (KRT18, RNAscope® Probe Hs-KRT18-C2, ACD Cat# 310211-C2) to detect epithelial cells, or CD68 to detect macrophages (RNAscope® Probe Hs-CD68-C2, ACD Cat# 560591-C2). In brief, FFPE slides were deparaffinized in xylene and ethanol followed by hydrogen peroxide treatment to block endogenous peroxidase activity (RNAscope® hydrogen peroxide, ACD, Cat# 322335), incubation in target retrieval solution for 15 min (RNAscope® Target Retrieval Reagents, ACD Cat# 322000), and proteolytic digestion for 30 min as pre-incubation procedures (RNAscope® Protease Plus, ACD Cat# 322331). The slides were then transferred into a pre-warmed humidity control tray (ACD) and incubated with either a mixture of Channel 1 and Channel 2 solutions for the Duplex Assay or the SARS-CoV-2-probe only in case of single probe detection. The humidity control tray was placed in a HybEZ oven (ACD) for 2 h of incubation at 40 °C. The slides were then washed two times using RNAscope washing buffer and returned to the oven for another 30 min after submersion in AMP-1 reagent. Washing and amplification steps were repeated using the AMP-2 to AMP-6 reagents with alternating 15-min and 30-min incubation periods, respectively. For single probe detection, the RED solution was prepared by mixing RED-A (RNAscope® Fast Red A, ACD Cat# 320458) and RED-B (RNAscope® Fast Red B, ACD Cat# 320459) in a ratio of 60:1. For signal visualization the RED solution was incubated for 10-min, followed by counterstaining with 50% hematoxylin and 0.05% ammonia. For dual probe detection, four additional amplification steps were performed before detecting the first probe using the RED solutions as describe above.

The second probe was visualized using the GREEN solutions (GREEN A (RNAscope® GREEN A, ACD Cat# 320718) plus GREEN B (RNAscope® GREEN B, ACD Cat# 320719), ratio 50:1). Counterstaining was performed as describe above for single probe detection. Each slide was examined by two pathologists (TL, CS). The overall viral load was semiquantitatively assessed by visual scoring using a four-tiered system (0 − 3): score 0 (no hybridization signal detected), score 1 (focal, isolated signals), score 2 (focal, piled signals) or score 3 (diffuse signals). In addition, the maximum number of double positive cells/mm^2 was counted in all cases showing a high viral load.

3. Results

3.1. Study cohort

During the recruitment period of the study 115 clinicopathological COVID-19 autopsies were performed at our institution. For this study, 40 patients of this cohort were selected and analyzed for presence and distribution of SARS-CoV-2 Spike protein-coding RNA in lung tissue. These included 28 patients infected by the original SARS-CoV-2 strain and 12 patients infected by different variants of concern (Alpha, B.1.1.7, n = 5; Delta, B.1.617.2, n = 5; Omicron, B.1.1.529, n = 2, respectively). The patientś characteristics are detailed in Table 1. The male to female ratio was 1.5–1. Median age at death was 79 years (range: 41–95 years). The mean duration of COVID-19, from onset to symptoms to death, was 10 days (range 0–31). In particular, ten of these patients died in less than one week, another nineteen during the second week, and the last eleven later than 14 days following disease onset. The mean duration of hospitalization was 7 days (range 0–36). Histological evaluation showed the previously reported pattern of lung damage over time with diffuse alveolar damage and alveolar edema observed in the exudative stage, followed by a proliferative stage characterized by pneumocyte hyperplasia, squamous metaplasia, and desquamation, and subsequently the development of an organizing pneumonia resulting in interstitial fibrosis (Fig. 1A-C) [13]. These pulmonary changes were considered the main cause of death in 26 patients. In the remaining twelve patients, autopsies revealed either bronchopneumonia related to super-infection (n = 6), myocardial infarction (n = 3), septic shock (n = 2), decompensated heart insufficiency (n = 1), pulmonary artery embolism (n = 1), or severe iron deficiency anemia (n = 1) as the underlying cause of death.

3.2. Detection of SARS-CoV-2 variants in situ

SARS-CoV-2 viral RNA was visualized in lung tissues using a probe against the Spike protein coding RNA sequence. Positive signals were retrieved within hyaline membranes covering the alveolar spaces as well as in the cytoplasm of cells within the alveoli and the alveolar septa (Fig. 1D-I). Based on the semiquantitative assessment of the SARS-CoV-2 RNA-ISH, six cases revealed a high viral load (Fig. 1D), ten cases were characterized as intermediate (Fig. 1E), and 16 cases were classified as having a low viral load (Fig. 1 F). Overall, no SARS-CoV-2 virus RNA could be detected in the lung tissue sections of eight patients. As the signal abundance varied remarkably between the individual cases (Table 1), the study cohort was categorized according to disease duration (less than one week, one to two weeks, and more than two weeks, respectively), which revealed a significant inverse association between signal abundance and duration (Spearmaṅs rho: −0.51, p = 0.001). In particular, the viral load was significantly reduced in cases with a disease duration more than 2 weeks compared to the other two subgroups ($p < 0.05$, Fig. 2 A). Six patients of this cohort had received a primary

Table 1
Patients characteristics.

ID	Age	Sex	Primary vaccination completed	Duration (d)	VOC	Co-morbidities	Mechanical ventilation	Viral load (ISH)	Disease stage	Cause of death
1	41	m	no	12	No	FLD	declined	3	exudative	COVID-19
2	89	f	no	2	No	AH, CAD	declined	0	exudative	COVID-19
3	81	m	no	15	No	AH, DM	declined	1	NA	bronchopneumonia
4	71	m	no	4	No	AH, DCMP	declined	1	exudative	myocardial insufficiency
5	77	f	no	5	No	AH, CAD, COPD	no	2	NA	bronchopneumonia
6	95	m	no	5	No	AH, ILD	declined	3	exudative	COVID-19
7	73	f	no	10	No	AH, MN, RA	declined	2	proliferating	COVID-19
8	81	f	no	5	No	AH, CAD, COPD, MetS	declined	1	fibrosing	COVID-19
9	89	m	no	8	No	AH, COPD	declined	2	exudative	COVID-19
10	78	m	no	6	No	AH, CAD, COPD, MN	declined	2	exudative	COVID-19
11	80	m	no	7	No	AH, COPD	no	2	exudative	COVID-19
12	60	f	no	8	No	AH, ILD	yes	3	proliferating	COVID-19
13	79	m	no	9	No	AH, COPD, MDS	declined	2	exudative	COVID-19
14	82	m	no	11	No	AH, DM	declined	1	exudative	septic multiorganfailure
15	78	f	no	9	No	AH, DM	yes	1	fibrosing	septic multiorganfailure
16	79	f	no	10	No	DCMP, MN, PH, SMF	declined	1	fibrosing	COVID-19
17	86	f	no	11	No	AH, CAD, COPD, DM, RI	declined	1	exudative	COVID-19
18	90	f	no	11	No	AH, DM, MetS, RI	declined	0	fibrosing	COVID-19
19	69	m	no	15	B.1.1.7	AH, DM, S	yes	0	fibrosing	Myocardial infarction
20	66	m	no	31	No	CLL, COPD	yes	1	proliferating	COVID-19
21	86	m	no	8	No	AH, CAD, COPD, MN	declined	2	proliferating	COVID-19
22	86	f	no	14	No	AH, MN	declined	1	proliferating	bronchopneumonia
23	93	f	no	15	No	AH, CAD, RI	declined	1	exudative	myocardial infarction
24	78	m	no	15	No	AH	yes	1	fibrosing	COVID-19
25	78	m	no	16	No	AH	yes	0	fibrosing	COVID-19
26	65	m	no	18	B.1.1.7	AH, CAD, DM, MetS	yes	1	fibrosing	myocardial infarction
27	91	m	no	19	No	AH, RI	declined	0	fibrosing	COVID-19
28	61	f	no	23	No	AH, MetS	yes	0	exsudative	COVID-19
29	79	m	no	22	No	AH, CAD, COPD, DM	yes	0	fibrosing	COVID-19
30	59	m	no	27	No	AH, CAD, SA	yes	1	fibrosing	bronchopneumonia
31	91	m	yes	6	B.1.1.7	AH, CAD, COPD, S	declined	2	exsudative	COVID-19
32	74	m	no	9	B.1.1.7	CAD, K, MN	declined	3	proliferating	COVID-19
33	68	f	no	12	B.1.1.7	AH, LC, RA	yes	2	fibrosing	bronchopneumonia
34	65	m	yes	4	B.1.617.2	AH, CAD, MetS, S	yes	2	exsudative	COVID-19
35	80	f	yes	1	B.1.617.2	AH, CAD, COPD, NSCLC, paraplegia	declined	3	exsudative	bronchopneumonia
36	88	m	yes	0	B.1.617.2	AH	yes	1	exsudative	Iron deficiency anemia
37	74	f	no	12	B.1.1.529	AH, CAD, MN, NF	yes	1	exsudative	COVID-19
38	72	f	no	8	B.1.617.2	GBM	no	3	exsudative	COVID-19 & end-stage cancer
39	81	m	yes	8	B.1.617.2	AH, CAD	yes	1	fibrosing	COVID-19
40	87	m	yes	12	B.1.1.529	CAD, COPD	yes	0	fibrosing	Pulmonary artery embolism

Abbreviations: AH, arterial hypertension; CAD, coronary artery disease; COPD, chronic obstructive pulmonary disease; DCMP, dilatative cardiomyopathy; f, female; FLD, fatty liver disease; GBM, glioblastoma multiforme, ILD, interstitial lung disease; K, kyphoscoliosis; LC, liver cirrhosis; m, male; MDS, myelodysplastic syndrome; METS, metabolic syndrome; MN, malnutrition; NA, not applicable; NF1, neurofibromatosis type 1; NSCLC, non-small cell lung cancer; PH, pulmonary hypertension; RA, rheumatoid arthritis, RI, renal insufficiency; S, sarcoidosis; SMF, secondary myelofibrosis; T2DM, type 2 diabetes mellitus; VOC, variant of concern

vaccination series. At least in this cohort of deceased COVID-19 patients, the viral load (as determined by semiquantitative evaluation) was not significantly different between vaccinated or non-vaccinated cases ($p > 0.05$, Fig. 2B).

Regarding virus variants, our diagnostic approach detected 89% ($n = 16/18$) of the cases infected by the original virus strain and 80% ($n = 4/5$), 100% ($n = 5$), and 50% ($n = 1/2$) of cases infected by the Alpha (B.1.1.7), Delta (B.1.617.2), and Omicron (B.1.1.529) variants, respectively.

Histological analysis of the lung tissue sections showed only the early exudative stage of COVID-19 pneumonia in 18 patients, the additional presence of proliferative stage features was seen in six patients, and areas of late disease with interstitial fibroses were evident in 14 patients (Fig. 1A-C). Two patients could not be adequately categorized due to severe overlapping bronchopneumonia. Again, an inverse correlation between signal abundance and the stage of COVID-19 pneumonia was noted (Spearmanś rho: −0.46, $p = 0.004$), which was paralleled by a positive association between disease duration and disease stage (Spearmanś rho: 0.49, $p = 0.002$). In line with this, less viral load was seen in the fibrosing stage of COVID-19 pneumonia compared to the exudative or the proliferating disease stage ($p < 0.05$, Fig. 2 C).

Patientś with fatal outcome after SARS-CoV-2 infection are frequently older males with existing co-morbidities like arterial hypertension, chronic obstructive pulmonary disease (COPD), and type 2 diabetes mellitus (T2DM) [13]. There was no statistical association between abundance of viral RNA in lung tissue and age, sex, presence of arterial hypertension or COPD, mechanical ventilation or COVID-19-related death (each $p > 0.05$), but the abundance of SARS-CoV-2 signals in lung tissue was significantly less in patients with known T2DM ($p = 0.01$).

3.3. *Lung endothelial cells are not a major target of SARS-CoV-2*

In order to depict the cell types, which were infected by SARS-CoV-2, dual RNA-ISH were performed. Intracellular SARS-CoV-2 In cases with high viral load, Spike-coding RNA signals were predominantly detected in keratin 18 (KRT18; median 6 positive cells/mm^2, range 5–10; Supplementary Table 1) RNA positive pneumocytes (Fig. 1 G) and CD68

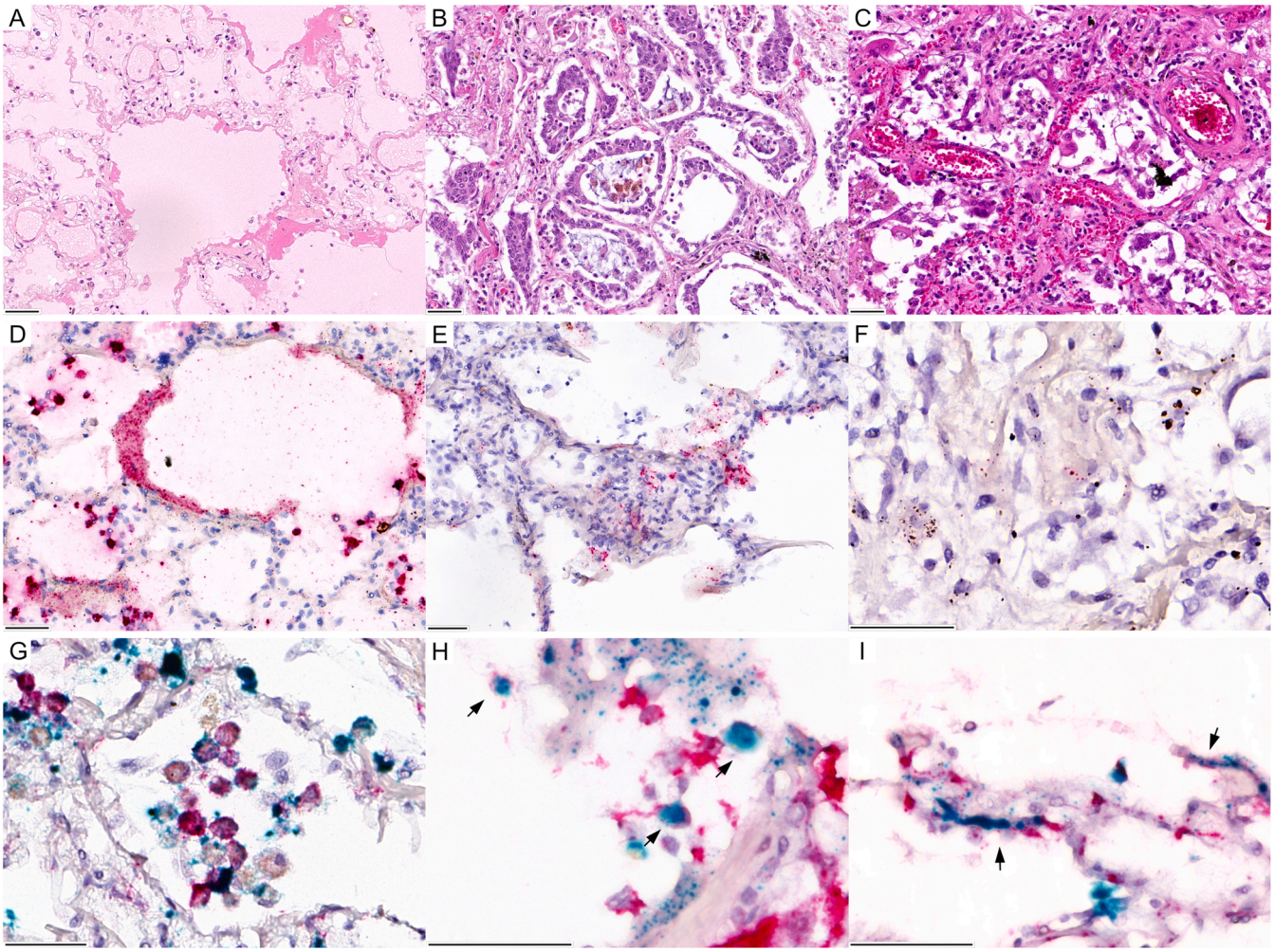

Fig. 1. Temporal course of SARS-CoV-2 lung infection, A) Early COVID-19 pneumonia showing alveolar edema and hyaline membrane formation. B) Intermediate proliferative stage of COVID-19 pneumonia with type II pneumocyte hyperplasia and squamous metaplasia. C) Late stage disease with coexistence of alveolar macrophages accumulation, type II pneumocyte hyperplasia and septal broadening due to interstitial fibrosis. D) Same patient as in A, diffuse SARS-CoV2-Spike RNA signals (red) in alveolar cells and hyaline membrane. E) Same patient as in B, focal piling of SARS-CoV2-Spike RNA signals (red) in alveolar and interstitial cells. F) Same patient as in C, focal detection of single hybridization signals (red) in this case. G) CD68 RNA positive macrophages (red) are packed with SARS-CoV-2 Spike RNA (green). H) Co-hybridization with a KRT18 probe (red) demonstrates presence of viral RNA (green) in pneumocytes (arrows). I) Very few Spike RNA signals (green) are seen in MCAM RNA (red) positive endothelial cells (arrows). I) Each bar represents 50 μm.

molecule (CD68; median 17 positive cells/mm^2, range 10–29) RNA expressing alveolar macrophages (Fig. 1I). A SARS-CoV-2 RNA signal was significantly less frequently detected in Melanoma Cell Adhesion Molecule (MCAM) RNA-positive endothelial cells (Fig. 1H). In these cases, only isolated viral transcripts could be detected even in cases with high viral load (median 1 positive cells/mm^2, range 0–1; Fig. 2D). In addition, viral RNA was present in hyaline membranes covering the alveolar spaces in 11 cases (Fig. 1D).

4. Discussion

The interaction of the viral Spike protein with cellular receptors (*e.g.* ACE2, TMPRSS2, and others) allows SARS-CoV-2 to efficiently enter its target cells [17,27]. These receptors are not only present on lung epithelial cells, but have also been reported to be consistently expressed by endothelial cells [10].

In line with the high expression of SARS-CoV-2 receptors in lung epithelial cells, SARS-CoV-2 Spike protein coding RNA was detected in KRT18 RNA expressing lung epithelial cells. As viral RNA is generated during viral replication in infected cells, the presence of viral RNA in hyaline membranes may be explained by death or lysis of infected epithelial cells. SARS-CoV-2 infection has been shown to exert variable cytopathogenic effects, ranging from lysis of the infected cells to no cytopathic effect in spite of intense viral replication [29]. This is in line with electron microscopy observations showing that new SARS-CoV-2 particles were expelled from the cells, through cell lysis or by fusion of virus containing vacuoles with the cell plasma membrane [3]. Alternatively, release of viral RNA may be related to the host's immune cells attacking infected cells. However, viral particles present in the alveolar spaces will be included during aerosol and droplet generation and will thus be shed by patients with active viral replication during breathing and talking [5] suggesting that detectable viral RNA in the alveolar spaces may also be considered as a surrogate of patient's infectivity. However, we cannot reliably determine the source of the viral RNA detected extracellularly in the hyaline membranes. Besides direct viral infection a concurrent explanation for the presence of viral RNA in alveolar macrophages (expressing CD68 RNA) could be phagocytosis of alveolar debris.

As autopsy studies revealed focal capillary microthrombosis and vascular dysfunction as the most likely factor leading to alveolar damage and consequently lung fibrosis during SARS-CoV-2 lung infection [13,18], the observation that endothelial cells also express SARS-CoV-2

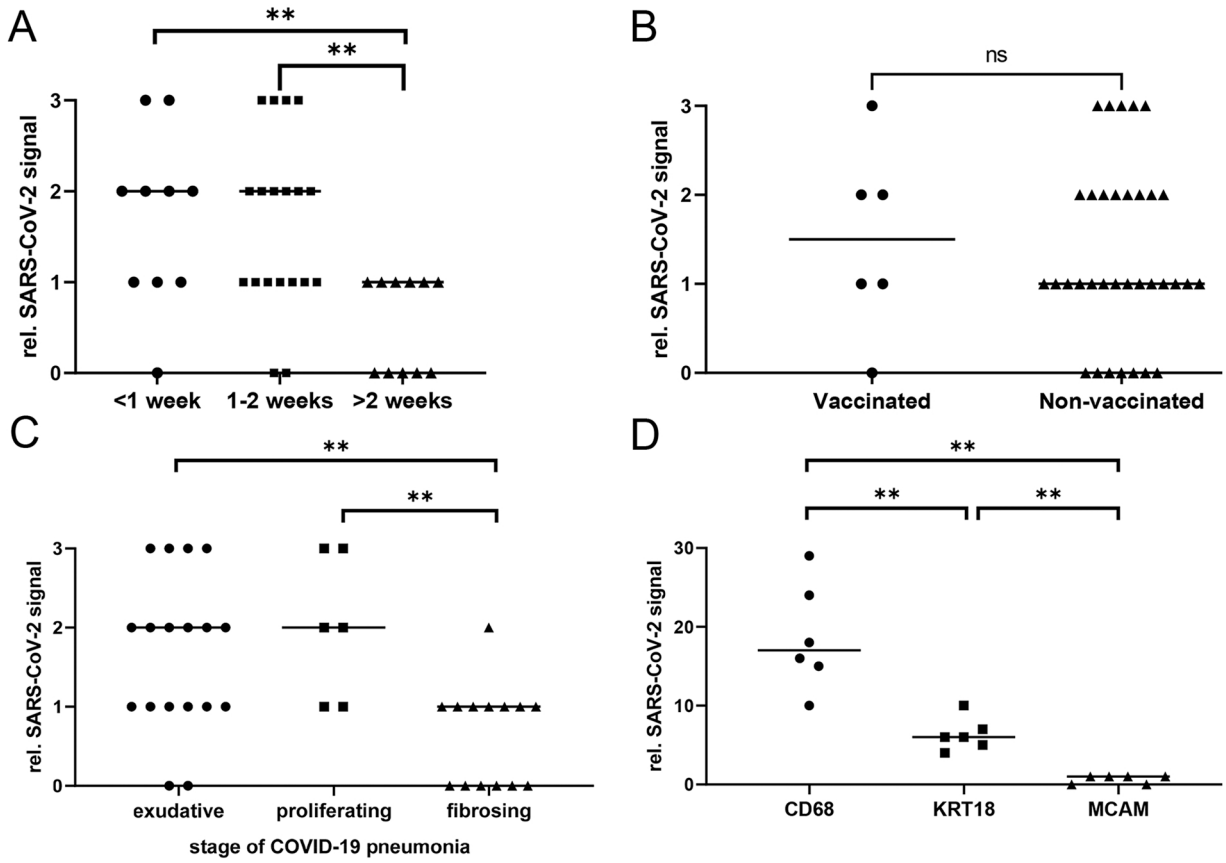

Fig. 2. Quantification of viral RNA in lung tissue A) Clearance of viral RNA from lung tissue over time. B) Comparison of SARS-CoV-2 RNA signals in deceased COVID-19 patients with and without prior anti-SARS-CoV-2 vaccination. C) Viral RNA signals in different stages of COVID-19 pneumonia. D) Quantification of viral RNA in different cell types. CD68 marks alveolar macrophages. KRT 18 was used to detect lung epithelial cells and MCAM was used to identify SARS-CoV-2 in endothelial cells. *$p < 0.05$; **$p < 0.01$; ns, not significant.

receptors could be of special interest [10]. Noteworthy, initial reports demonstrated SARS-CoV-2 viral particles in renal but not lung endothelial cells [18,26], while others suggested a misinterpretation of autolytically altered cellular organelles as viral particles [9]. We were not able to reliably detect viral particles by electron microscopy in lung endothelial cells using tissues retrieved from autopsies of COVID-19 patients (data not shown). Similarly, Cortese at al. were not able to detect SARS-CoV-2 in lung endothelial cells and Stahl et al. did not find SARS-CoV-2 infected endothelial cells in the gut [7,24]. Thus, we decided for an alternate diagnostic approach allowing for the analysis of larger tissue areas. Indeed, we were able to identify single virus-positive endothelial cells using dual RNA *in situ* hybridization in cases with high viral load (Fig. 1H), but the vast majority of the examined cases were negative for SARS-CoV-2 RNA in lung endothelial cells. As COVID-19-related lung damage was histologically present in nearly all of our patients (n = 38/40), it seems unlikely that direct viral infection of lung endothelial cells is key for the induction of capillary microthrombosis. In line with this finding, platelets have been shown to express both ACE2 and TMPRSS2 and the viral Spike protein was able to directly enhance platelet activation [33] suggesting that altered platelet function itself might be involved in the pathogenesis of thrombotic events during severe COVID-19.

Other striking findings in lungs of deceased COVID-19 patients include morphological changes affecting type II pneumocytes like hyperplasia, multinucleation, and squamous metaplasia besides accumulation of alveolar macrophages [4,13,31]. Here, we demonstrated the presence of SARS-CoV-2 RNA in lung epithelial cells and alveolar macrophages. Interestingly, spatial transcriptomics suggested that squamous metaplasia may be an important feature of SARS-CoV-2 pneumonia and revealed that SARS-CoV-2 infection may increase epithelial-to-mesenchymal transition besides activation of extracellular matrix pathways [16]. These transcriptomic analyses also pointed to the direction that SARS-CoV-2 macrophages are alternatively activated and may contribute to tissue remodeling during COVID-19 pneumonia. Taken together, these findings suggest that the infection of lung epithelial cells may directly affect the function of the air-blood barrier and may together with virus containing alveolar macrophages contribute to progressive lung fibrosis in patients with severe COVID-19 [31].

The duration of infectivity of SARS-CoV-2 infected people has major implications for public health and duration of quarantine measures used for pandemic control. Viral RNA is detectable in nasopharyngeal swabs 2–3 days before onset of symptoms at which viral titers peak, and decline over the following 7–8 days in most patients [11,25,28]. However, there are some patients in which viral RNA can be detected for weeks and months [20,23,32], which cannot be considered as a general surrogate of infectivity [22]. Similar results have been reported from animal models [2,21]. Initially, the duration of viral shedding and thus the contagious period of SARS-CoV-2 infected patients has been reported to last about three weeks [19,30], but vaccination has shown to reduce the time to viral clearance [6]. Here, we observed a steady decrease in SARS-CoV-2 Spike protein-coding RNA signals in lung tissue over a period of three weeks, which is similar to the data provided by Desai et al. [8] and consistent with the reported periods of viral shedding in a non-vaccinated population. Interestingly, high and persistent SARS-CoV-2 shedding in the lower respiratory tract has been associated with a severe course of COVID-19 [5], which was the case in most of our patients. Noteworthy, we did not observe a significant difference in viral

load between vaccinated and non-vaccinated patients with fatal COVID-19 ($p > 0.05$). Whether this may be attributable to the low number of deceased vaccinated COVID-19 patients in our cohort or related to the fact of disease fatality remains a subject for future analysis.

5. Conclusions

We characterized the natural course of viral clearance of SARS-CoV-2 RNA in lung tissue of adults with severe COVID-19 and fatal outcome. Furthermore, we demonstrated that variants of concern can be detected using the described RNA *in situ* hybridization approach. Our observations indicate that pulmonary microthrombosis, a known driver of disease progression, is likely not a direct consequence of endothelial cells infection.

CRediT authorship contribution statement

Constantin Schwab: Data curation, Formal analysis, Investigation, Methodology, Writing – original draft. **Lisa Maria Domke**: Data curation, Funding acquisition, Project administration, Review and editing draft. **Fabian Rose**: Formal analysis, Investigation, Methodology, Review and editing draft. **Ingrid Hausser**: Investigation, Methodology, Review and editing draft. **Peter Schirmacher**: Funding acquisition, Supervision, Review and editing draft. **Thomas Longerich**: Conceptualization, Funding acquisition, Investigation, Methodology, Project administration, Supervision, Review and editing draft.

Funding

The study was funded by the Ministry of Science, Research and Art of Baden-Wuerttemberg (Baden-Wuerttemberg Corona Autopsy Biobank and Registry and "Sonderfördermaßnahme COVID-19 Forschung", HD14 to TL).

Declaration of Competing Interest

The authors declare that they have no known competing financial interests or personal relationships that could have appeared to influence the work reported in this paper.

Acknowledgements

We thank Martin Bär and his team for supporting the COVID-19 autopsies and the biobank of the German Center for Infection Research (Deutsches Zentrum für Infektionsforschung, DZIF) for the procurement and administration of tissue samples

Appendix A. Supporting information

Supplementary data associated with this article can be found in the online version at doi:10.1016/j.prp.2022.154000.

References

[1] M. Ackermann, S.E. Verleden, M. Kuehnel, A. Haverich, T. Welte, F. Laenger, A. Vanstapel, C. Werlein, H. Stark, A. Tzankov, W.W. Li, V.W. Li, S.J. Mentzer, D. Jonigk, Pulmonary vascular endothelialitis, thrombosis, and angiogenesis in Covid-19, N. Engl. J. Med. 383 (2020) 120–128.

[2] L. Bao, W. Deng, B. Huang, H. Gao, J. Liu, L. Ren, Q. Wei, P. Yu, Y. Xu, F. Qi, Y. Qu, F. Li, Q. Lv, W. Wang, J. Xue, S. Gong, M. Liu, G. Wang, S. Wang, Z. Song, L. Zhao, P. Liu, L. Zhao, F. Ye, H. Wang, W. Zhou, N. Zhu, W. Zhen, H. Yu, X. Zhang, L. Guo, L. Chen, C. Wang, Y. Wang, X. Wang, Y. Xiao, Q. Sun, H. Liu, F. Zhu, C. Ma, L. Yan, M. Yang, J. Han, W. Xu, W. Tan, X. Peng, Q. Jin, G. Wu, C. Qin, The pathogenicity of SARS-CoV-2 in hACE2 transgenic mice, Nature 583 (2020) 830–833.

[3] D. Brahim Belhaouari, A. Fontanini, J.P. Baudoin, G. Haddad, M. Le Bideau, J. Y. Bou Khalil, D. Raoult, B. La Scola, The strengths of scanning electron microscopy in deciphering SARS-CoV-2 infectious cycle, Front. Microbiol. 11 (2020) 2014.

[4] L. Carsana, A. Sonzogni, A. Nasr, R.S. Rossi, A. Pellegrinelli, P. Zerbi, R. Rech, R. Colombo, S. Antinori, M. Corbellino, M. Galli, E. Catena, A. Tosoni, A. Gianatti, M. Nebuloni, Pulmonary post-mortem findings in a series of COVID-19 cases from northern Italy: a two-centre descriptive study, Lancet Infect. Dis. 20 (2020) 1135–1140.

[5] P.Z. Chen, N. Bobrovitz, Z.A. Premji, M. Koopmans, D.N. Fisman, F.X. Gu, SARS-CoV-2 shedding dynamics across the respiratory tract, sex, and disease severity for adult and pediatric COVID-19, Elife 10 (2021).

[6] L. Coppeta, O. Balbi, Z. Grattagliano, G.G. Mina, A. Pietroiusti, A. Magrini, M. Bolcato, M. Trabucco Aurilio, First dose of the BNT162b2 mRNA COVID-19 vaccine reduces symptom duration and viral clearance in healthcare workers, Vaccines 9 (2021).

[7] K. Cortese, G. Holland, L. Möller, M.C. Gagliani, E. Barisione, L. Ball, P. Pelosi, F. Grillo, L. Mastracci, R. Fiocca, M. Laue, Ultrastructural examination of lung "cryobiopsies" from a series of fatal COVID-19 cases hardly revealed infected cells, Virchows Arch. Int. J. Pathol. (2022) 1–11.

[8] N. Desai, A. Neyaz, A. Szabolcs, A.R. Shih, J.H. Chen, V. Thapar, L.T. Nieman, A. Solovyov, A. Mehta, D.J. Lieb, A.S. Kulkarni, C. Jaicks, K.H. Xu, M.J. Raabe, C. J. Pinto, D. Juric, I. Chebib, R.B. Colvin, A.Y. Kim, R. Monroe, S.E. Warren, P. Danaher, J.W. Reeves, J. Gong, E.H. Rueckert, B.D. Greenbaum, N. Hacohen, S. M. Lagana, M.N. Rivera, L.M. Sholl, J.R. Stone, D.T. Ting, V. Deshpande, Temporal and spatial heterogeneity of host response to SARS-CoV-2 pulmonary infection, Nat. Commun. 11 (2020) 6319.

[9] C.S. Goldsmith, S.E. Miller, R.B. Martines, H.A. Bullock, S.R. Zaki, Electron microscopy of SARS-CoV-2: a challenging task, Lancet 395 (2020), e99.

[10] I. Hamming, W. Timens, M.L. Bulthuis, A.T. Lely, G. Navis, H. van Goor, Tissue distribution of ACE2 protein, the functional receptor for SARS coronavirus. A first step in understanding SARS pathogenesis, J. Pathol. 203 (2004) 631–637.

[11] X. He, E.H.Y. Lau, P. Wu, X. Deng, J. Wang, X. Hao, Y.C. Lau, J.Y. Wong, Y. Guan, X. Tan, X. Mo, Y. Chen, B. Liao, W. Chen, F. Hu, Q. Zhang, M. Zhong, Y. Wu, L. Zhao, F. Zhang, B.J. Cowling, F. Li, G.M. Leung, Temporal dynamics in viral shedding and transmissibility of COVID-19, Nat. Med. 26 (2020) 672–675.

[12] B. Hu, H. Guo, P. Zhou, Z.L. Shi, Characteristics of SARS-CoV-2 and COVID-19, Nat. Rev. Microbiol. 19 (2021) 141–154.

[13] F.K.F. Kommoss, C. Schwab, L. Tavernar, J. Schreck, W.L. Wagner, U. Merle, D. Jonigk, P. Schirmacher, T. Longerich, The pathology of severe COVID-19-related lung damage, Dtsch. Arzteblatt Int. 117 (2020) 500–506.

[14] F. Liu, K. Han, R. Blair, K. Kenst, Z. Qin, B. Upcin, P. Wörsdörfer, C.C. Midkiff, J. Mudd, E. Belyaeva, N.S. Milligan, T.D. Rorison, N. Wagner, J. Bodem, L. Dölken, B.H. Aktas, R.S. Vander Heide, X.M. Yin, J.K. Kolls, C.J. Roy, J. Rappaport, S. Ergün, X. Qin, SARS-CoV-2 infects endothelial cells in vivo and in vitro, Front. Cell. Infect. Microbiol. 11 (2021), 701278.

[15] J. Liu, Y. Li, Q. Liu, Q. Yao, X. Wang, H. Zhang, R. Chen, L. Ren, J. Min, F. Deng, B. Yan, L. Liu, Z. Hu, M. Wang, Y. Zhou, SARS-CoV-2 cell tropism and multiorgan infection, Cell Discov. 7 (2021) 17.

[16] C. Margaroli, P. Benson, N.S. Sharma, M.C. Madison, S.W. Robison, N. Arora, K. Ton, Y. Liang, L. Zhang, R.P. Patel, A. Gaggar, Spatial mapping of SARS-CoV-2 and H1N1 lung injury identifies differential transcriptional signatures, Cell Rep. Med. 2 (2021), 100242.

[17] S. Matsuyama, N. Nao, K. Shirato, M. Kawase, S. Saito, I. Takayama, N. Nagata, T. Sekizuka, H. Katoh, F. Kato, M. Sakata, M. Tahara, S. Kutsuna, N. Ohmagari, M. Kuroda, T. Suzuki, T. Kageyama, M. Takeda, Enhanced isolation of SARS-CoV-2 by TMPRSS2-expressing cells, Proc. Natl. Acad. Sci. USA 117 (2020) 7001–7003.

[18] T. Menter, J.D. Haslbauer, R. Nienhold, S. Savic, H. Hopfer, N. Deigendesch, S. Frank, D. Turek, N. Willi, H. Pargger, S. Bassetti, J.D. Leuppi, G. Cathomas, M. Tolnay, K.D. Mertz, A. Tzankov, Postmortem examination of COVID-19 patients reveals diffuse alveolar damage with severe capillary congestion and variegated findings in lungs and other organs suggesting vascular dysfunction, Histopathology 77 (2020) 198–209.

[19] Y. Miyamae, T. Hayashi, H. Yonezawa, J. Fujihara, Y. Matsumoto, T. Ito, T. Tsubota, K. Ishii, Duration of viral shedding in asymptomatic or mild cases of novel coronavirus disease 2019 (COVID-19) from a cruise ship: a single-hospital experience in Tokyo, Japan, Int. J. Infect. Dis. IJID Off. Publ. Int. Soc. Infect. Dis. 97 (2020) 293–295.

[20] S.Y. Park, S.G. Yun, J.W. Shin, B.Y. Lee, H.J. Son, S. Lee, E. Lee, T.H. Kim, Persistent severe acute respiratory syndrome coronavirus 2 detection after resolution of coronavirus disease 2019-associated symptoms/signs, Korean J. Intern. Med. 35 (2020) 793–796.

[21] B. Rockx, T. Kuiken, S. Herfst, T. Bestebroer, M.M. Lamers, B.B. Oude Munnink, D. de Meulder, G. van Amerongen, J. van den Brand, N.M.A. Okba, D. Schipper, P. van Run, L. Leijten, R. Sikkema, E. Verschoor, B. Verstrepen, W. Bogers, J. Langermans, C. Drosten, M. Fentener van Vlissingen, R. Fouchier, R. de Swart, M. Koopmans, B.L. Haagmans, Comparative pathogenesis of COVID-19, MERS, and SARS in a nonhuman primate model, Science 368 (2020) 1012–1015.

[22] E.V. Shidlovskaya, N.A. Kuznetsova, E.V. Divisenko, M.A. Nikiforova, A. E. Siniavin, D.A. Ogarkova, A.V. Shagaev, M.A. Semashko, A.P. Tkachuk, O. A. Burgasova, V.A. Gushchin, The value of rapid antigen tests for identifying carriers of viable SARS-CoV-2, Viruses 13 (2021).

[23] K.H. Song, D.M. Kim, H. Lee, S.Y. Ham, S.M. Oh, H. Jeong, J. Jung, C.K. Kang, J. Y. Park, Y.M. Kang, J.Y. Kim, J.S. Park, K.U. Park, E.S. Kim, H.B. Kim, Dynamics of viral load and anti-SARS-CoV-2 antibodies in patients with positive RT-PCR results after recovery from COVID-19, Korean J. Intern. Med. 36 (2021) 11–14.

[24] K. Stahl, J.H. Bräsen, M.M. Hoeper, S. David, Absence of SARS-CoV-2 RNA in COVID-19-associated intestinal endothelialitis, Intensive Care Med. 47 (2021) 359–360.

[25] K.K. To, O.T. Tsang, W.S. Leung, A.R. Tam, T.C. Wu, D.C. Lung, C.C. Yip, J.P. Cai, J. M. Chan, T.S. Chik, D.P. Lau, C.Y. Choi, L.L. Chen, W.M. Chan, K.H. Chan, J.D. Ip, A.C. Ng, R.W. Poon, C.T. Luo, V.C. Cheng, J.F. Chan, I.F. Hung, Z. Chen, H. Chen,

K.Y. Yuen, Temporal profiles of viral load in posterior oropharyngeal saliva samples and serum antibody responses during infection by SARS-CoV-2: an observational cohort study, Lancet Infect. Dis. 20 (2020) 565–574.
[26] Z. Varga, A.J. Flammer, P. Steiger, M. Haberecker, R. Andermatt, A.S. Zinkernagel, M.R. Mehra, R.A. Schuepbach, F. Ruschitzka, H. Moch, Endothelial cell infection and endotheliitis in COVID-19, Lancet 395 (2020) 1417–1418.
[27] Q. Wang, Y. Zhang, L. Wu, S. Niu, C. Song, Z. Zhang, G. Lu, C. Qiao, Y. Hu, K. Y. Yuen, Q. Wang, H. Zhou, J. Yan, J. Qi, Structural and functional basis of SARS-CoV-2 entry by using human ACE2, Cell 181 (2020) 894–904, e899.
[28] R. Wölfel, V.M. Corman, W. Guggemos, M. Seilmaier, S. Zange, M.A. Müller, D. Niemeyer, T.C. Jones, P. Vollmar, C. Rothe, M. Hoelscher, T. Bleicker, S. Brünink, J. Schneider, R. Ehmann, K. Zwirglmaier, C. Drosten, C. Wendtner, Virological assessment of hospitalized patients with COVID-2019, Nature 581 (2020) 465–469.
[29] N. Wurtz, G. Penant, P. Jardot, N. Duclos, B. La Scola, Culture of SARS-CoV-2 in a panel of laboratory cell lines, permissivity, and differences in growth profile, Eur. J. Clin. Microbiol. Infect. Dis. 40 (2021) 477–484.
[30] A.T. Xiao, Y.X. Tong, C. Gao, L. Zhu, Y.J. Zhang, S. Zhang, Dynamic profile of RT-PCR findings from 301 COVID-19 patients in Wuhan, China: a descriptive study, J. Clin. Virol. Off. Publ. Pan Am. Soc. Clin. Virol. 127 (2020), 104346.
[31] X.H. Yao, T. Luo, Y. Shi, Z.C. He, R. Tang, P.P. Zhang, J. Cai, X.D. Zhou, D.P. Jiang, X.C. Fei, X.Q. Huang, L. Zhao, H. Zhang, H.B. Wu, Y. Ren, Z.H. Liu, H.R. Zhang, C. Chen, W.J. Fu, H. Li, X.Y. Xia, R. Chen, Y. Wang, X.D. Liu, C.L. Yin, Z.X. Yan, J. Wang, R. Jing, T.S. Li, W.Q. Li, C.F. Wang, Y.Q. Ding, Q. Mao, D.Y. Zhang, S. Y. Zhang, Y.F. Ping, X.W. Bian, A cohort autopsy study defines COVID-19 systemic pathogenesis, Cell Res. 31 (2021) 836–846.
[32] F. Yu, L. Yan, N. Wang, S. Yang, L. Wang, Y. Tang, G. Gao, S. Wang, C. Ma, R. Xie, F. Wang, C. Tan, L. Zhu, Y. Guo, F. Zhang, Quantitative detection and viral load analysis of SARS-CoV-2 in infected patients, Clin. Infect. Dis. Off. Publ. Infect. Dis. Soc. Am. 71 (2020) 793–798.
[33] S. Zhang, Y. Liu, X. Wang, L. Yang, H. Li, Y. Wang, M. Liu, X. Zhao, Y. Xie, Y. Yang, S. Zhang, Z. Fan, J. Dong, Z. Yuan, Z. Ding, Y. Zhang, L. Hu, SARS-CoV-2 binds platelet ACE2 to enhance thrombosis in COVID-19, J. Hematol. Oncol. 13 (2020) 120.